ECCOMAS Congress 2016
VII European Congress on Computational Methods in Applied Sciences and Engineering
M. Papadrakakis, V. Papadopoulos, G. Stefanou, V. Plevris (eds.)
Crete Island, Greece, 5–10 June 2016

NUMERICAL MODELLING OF SURFACE WAVES IN THE FRAMEWORK OF SHALLOW WATER MODEL

Nina Shokina[1], **Gayaz Khakimzyanov**[2]

[1]Computing Center, University of Freiburg
Hermann-Herder-Straße 10, 79104 Freiburg im Breisgau, Germany
e-mail: nina.shokina@gmail.com

[2] Institute of Computational Technologies SB RAS
Lavrentiev Ave. 6, 630090 Novosibirsk, Russia
e-mail: khak@ict.nsc.ru

Keywords: Nonlinear Shallow Water Equations, Finite-Difference Scheme, Adaptive Grid, Surface Waves, Run-Up

Abstract. *An improved adaptive grid method is considered for the numerical solution of the problems on propagation and run-up of surface waves, described by the one-dimensional shallow water model. The modified algorithm for the realization of the explicit predictor-corrector scheme is presented, which is based on the new way of computation of the right-hand side of the shallow water equations. A new method for choosing the scheme parameters on the basis of the analysis of the differential approximation is suggested that guarantees the satisfaction of the TVD-property for the improved predictor-corrector scheme. The presented method for construction of different conservative schemes on moving grids is based on an appropriate choice of the scheme parameters for the predictor–corrector scheme, which represents the canonical form of the two-layer explicit schemes for the shallow water equations. The improved difference boundary conditions are obtained at the moving waterfront point using the known analytical solutions of the shallow water equations in the vicinity of a water-land boundary. These boundary conditions approximate the analytical solutions with a higher accuracy than the conditions used in the earlier works. The numerical results for the improved adaptive grid method are presented.*

1 INTRODUCTION

Nowadays, the methods based on the hierarchy of embedded mathematical models [1] and computational algorithms are widely used for the numerical solution of the problems on propagation of long surface waves in large water areas and their interaction with coasts. The nonlinear shallow water models hold a central position in such a hierarchy. Therefore, the development and investigation of numerical methods for the solution of the problems in the framework of shallow water models is a vital task of the modern computational fluid dynamics [2].

The present work is the continuation of the investigations started in [3] and devoted to some problems of the numerical modelling in the framework of the nonlinear non-dispersive shallow water model (NLSW-model). The NLSW-system is inhomogeneous for an irregular bottom, therefore, many finite-difference schemes, which show good results for a flat bottom, loose the important property of preservation of simple analytical solutions of the NLSW-model [4]. This problem can be solved by a special approximation of the right-hand side of the impulse equation.

It is known, that the solution of the NLSW-equations can become discontinuous even for continuous initial data, often leading to oscillations of the numerical solution [5, 6, 7]. A new approach for choosing the scheme parameters is suggested, which is based on the investigation of the differential approximation of the scheme, guaranteeing the satisfaction of the TVD-property.

In [3] an important conservation property for schemes on moving grids for the nonlinear scalar equation has been achieved by a proper choice of a scheme parameter. In the present work, the same approach is used for automatic construction of conservative schemes for the shallow water equations on moving grids.

An adequate description of the waterfront behavior in the run-up area and a reliable method for the detection of inundation zones are needed in the problems of the propagation of long surface waves in large water areas and their interaction with coasts. The methods for numerical modelling of flooding-drying processes, necessary for the detection of inundation zone after a wave run-up on a coast, can be divided into two main groups [8]. First group consists of the shock-capturing methods with direct application of existing algorithms on fixed spatial grids, where a waterfront has to be evaluated at each time moment. Second group contains the methods on moving grids, which adapt so that a waterfront always coincides with a computational domain boundary. In flooding-drying problems the finite volume methods [9, 10], finite element methods [11, 12, 13], finite difference methods [14, 15], particle method [16] and others are used for the fluid flow modelling.

The present work uses moving adaptive grids for the detection of inundation zones, and a waterfront position is obtained using the exact analytical solutions of the NLSW-model in the waterfront vicinity in a time interval equal to a time step of a numerical scheme. The updated formulas are presented for evaluating a waterfront position and velocity. The results of the numerical modelling of a wave run-up on vertical wall and plane slope are presented.

2 NEW PROCEDURE FOR RIGHT-HAND SIDE COMPUTATION

In [3] a finite-difference scheme on moving grids was suggested and investigated for the one-dimensional shallow water equations:

$$\vec{u}_t + \vec{f}_x = \vec{G}, \tag{1}$$

where

$$\vec{u} = \begin{pmatrix} H \\ Hu \end{pmatrix}; \quad \vec{f}(\vec{u}) = \begin{pmatrix} Hu \\ Hu^2 + gH^2/2 \end{pmatrix}; \quad \vec{G}(x, \vec{u}) = \begin{pmatrix} 0 \\ gHh_x \end{pmatrix};$$

t is the time; $u(x,t)$ is the velocity; $\eta(x,t)$ is the deviation of free surface from a rest level; $h(x)$ is the bottom depth measured from a free surface at rest; $H = \eta + h$ is the full depth; g is the gravity acceleration. It is assumed that some initial boundary value problem is formulated for the system of equations (1) on the interval $x \in [0,\ l]$ and time interval $t \in [0,\ T]$.

The node coordinates of a moving grid, covering the interval $[0,\ l]$ at time moment $t = t^n$, are denoted by x_j^n $(j = 0, \ldots, N)$. These nodes are the images of the nodes q_j of a uniform grid with a step $h = 1/N$ on the interval $q \in [0,\ 1]$ under some non-degenerated mapping $x = x(q,t)$. In the predictor-corrector scheme [3] the flux vector in computed in cell centers on the predictor step:

$$\hat{\vec{f}}_{j+1/2} = \frac{\vec{f}_j^n + \vec{f}_{j+1}^n}{2} - \frac{\tau}{2}\Big(\frac{1}{J}\mathcal{R}\mathcal{D}\bar{\Lambda}(\bar{\Lambda}\vec{P} - \mathcal{L}\vec{G})\Big)_{j+1/2}^n. \tag{2}$$

Then the flux vector is used for computing the full depth H_j^{n+1} and impulse $(Hu)_j^{n+1}$ according the explicit formulas on the corrector step:

$$\frac{(J\vec{u})_j^{n+1} - (J\vec{u})_j^n}{\tau} + \frac{\Big(\hat{\vec{f}} - (x_t\vec{u})^n\Big)_{j+1/2} - \Big(\hat{\vec{f}} - (x_t\vec{u})^n\Big)_{j-1/2}}{h} = \vec{G}_j^*, \tag{3}$$

where τ is the time step; $\vec{f}_j^n = \vec{f}(\vec{u}_j^n)$; $\vec{P}_{j+1/2}^n = (\mathcal{L}\vec{u}_q)_{j+1/2}^n$;

$$\vec{u}_{j+1/2}^n = \frac{\vec{u}_j^n + \vec{u}_{j+1}^n}{2}, \quad \vec{u}_{q,j+1/2}^n = \frac{\vec{u}_{j+1}^n - \vec{u}_j^n}{h}; \quad x_{t,j}^n = \frac{x_j^{n+1} - x_j^n}{\tau}; \quad x_{t,j+1/2}^n = \frac{x_{t,j}^n + x_{t,j+1}^n}{2};$$

$$J_{j+1/2}^n = \frac{x_{j+1}^n - x_j^n}{h} = x_{q,j+1/2}^n; \quad J_j^n = \frac{J_{j+1/2}^n + J_{j-1/2}^n}{2}; \quad \vec{G}_{j+1/2}^n = \begin{pmatrix} 0 \\ g\,(Hh_q)_{j+1/2}^n \end{pmatrix};$$

$$h_{q,j+1/2}^n = \frac{h_{j+1}^n - h_j^n}{h}; \quad h_j^n = h(x_j^n).$$

The matrices $\mathcal{L}$, $\mathcal{R}$, $\bar{\Lambda}$ from the equation (2) are defined as:

$$\mathcal{L}_{j+1/2}^n = \frac{1}{(c_{j+1/2}^n)^2}\begin{pmatrix} -\lambda_{2,j+1/2}^n & 1 \\ -\lambda_{1,j+1/2}^n & 1 \end{pmatrix}, \quad \mathcal{R}_{j+1/2}^n = \frac{c_{j+1/2}^n}{2}\begin{pmatrix} -1 & 1 \\ -\lambda_{1,j+1/2}^n & \lambda_{2,j+1/2}^n \end{pmatrix},$$

$$\bar{\Lambda}_{j+1/2}^n = \Lambda_{j+1/2}^n - x_{t,j+1/2}^n\mathcal{E}, \quad \Lambda_{j+1/2}^n = \begin{pmatrix} \lambda_{1,j+1/2}^n & 0 \\ 0 & \lambda_{2,j+1/2}^n \end{pmatrix},$$

where $\mathcal{E}$ is the identity matrix; $\lambda_{k,j+1/2}^n$ $(k = 1, 2)$ are the eigenvalues of the matrix $\mathcal{A}_{j+1/2}^n$, which approximates the Jacobi matrix of the system (1):

$$\mathcal{A}_{j+1/2}^n = \begin{pmatrix} 0 & 1 \\ -u_j^n u_{j+1}^n + gH_{j+1/2}^n & 2u_{j+1/2}^n \end{pmatrix} = (\mathcal{R}\Lambda\mathcal{L})_{j+1/2}^n, \tag{4}$$

$$\lambda^n_{1,j+1/2} = (u-c)^n_{j+1/2}\,, \quad \lambda^n_{2,j+1/2} = (u+c)^n_{j+1/2}\,, \tag{5}$$

$$c^n_{j+1/2} = \sqrt{(u^n_{j+1/2})^2 - u^n_j u^n_{j+1} + gH^n_{j+1/2}} \geq \sqrt{gH^n_{j+1/2}} > 0\,.$$

For computing the elements of the diagonal matrix

$$\mathcal{D}^n_{j+1/2} = \begin{pmatrix} 1+\theta^1_{j+1/2} & 0 \\ 0 & 1+\theta^2_{j+1/2} \end{pmatrix}$$

the following formula for the scheme parameters was suggested in [3]:

$$\theta^k_{j+1/2} = \begin{cases} 0, & \left|g^k_{j+1/2}\right| \leq \left|g^k_{j+1/2-s_k}\right| \quad g^k_{j+1/2}\cdot g^k_{j+1/2-s_k} \geq 0, \\ \theta^k_{0,j+1/2}(1-\xi^k_{j+1/2}), & \left|g^k_{j+1/2}\right| > \left|g^k_{j+1/2-s_k}\right| \quad g^k_{j+1/2}\cdot g^k_{j+1/2-s_k} \geq 0, \\ \theta^k_{0,j+1/2}, & g^k_{j+1/2}\cdot g^k_{j+1/2-s_k} < 0, \end{cases} \tag{6}$$

where $k = 1, 2;\ \xi^k_{j+1/2} = g^k_{j+1/2-s_k}/g^k_{j+1/2};\ s_k \equiv s^n_{k,j+1/2} = \operatorname{sgn}\bar{\lambda}^n_{k,j+1/2}$;

$$g^k_{j+1/2} = \left(|\bar{\lambda}_k|(1-\mathrm{C}_k)p_k\right)^n_{j+1/2}; \quad \mathrm{C}^n_{k,j+1/2} = æ\Big(\frac{|\bar{\lambda}_k|}{J}\Big)^n_{j+1/2}; \quad \theta^k_{0,j+1/2} = \frac{1}{\mathrm{C}^n_{k,j+1/2}} - 1;$$

$p^n_{k,j+1/2}$ are the components of the vector $\vec{P}^n_{j+1/2}$; $\bar{\lambda}^n_{k,j+1/2} = \left(\lambda_k - x_t\right)^n_{j+1/2}$ are the diagonal matrices $\bar{\Lambda}^n_{j+1/2}$; $æ = \tau/h$. In the computations the modified formula (6) was used, obtained in [3] as the result of the entropy fix on the basis of the differential approximation method. This formula guarantees the non-negativity of approximation viscosity in the vicinity of the sonic point of depression wave.

The values $\mathrm{C}^n_{k,j+1/2}$ can be named as the local Courant numbers corresponding to the eigenvalues $\lambda^n_{k,j+1/2}$. As in the case of uniform fixed grids, the time step τ is chosen from considerations of stability of the computations on moving grids, meaning that the following condition should be fulfilled:

$$\max_{k,j} \mathrm{C}^n_{k,j+1/2} < 1.$$

In [3] the right-hand side of the equation (3) was computed as

$$\vec{G}^*_j = \begin{pmatrix} 0 \\ gH^*_j h^*_{q,j} \end{pmatrix}.$$

Therefore, one more equation had to be solved on the predictor step in addition to two equations of the system (2). This equation was obtained by the approximation of the first equation of the system (1) and used for computing the full depth H^*_j in integer nodes. For this additional equation, the values $\lambda^n_{k,j}$ and θ^k_j had to be evaluated in integer nodes using the complex formulas differing from (5), (6). These additional computations have been increasing the computational time for one-dimensional problems and especially – for two-dimensional problems.

Let us consider a more economic procedure for computing the right-hand side of the equation (3):

$$\vec{G}^*_j = \begin{pmatrix} 0 \\ g(Hh_q)^{n+1/2}_j \end{pmatrix}, \tag{7}$$

where

$$H_j^{n+1/2} = \frac{H_{j+1}^{n+1} + H_{j-1}^{n+1} + H_{j+1}^{n} + H_{j-1}^{n}}{4}; \quad h_{q,j}^{n+1/2} = \frac{h_{j+1}^{n+1} - h_{j-1}^{n+1} + h_{j+1}^{n} - h_{j-1}^{n}}{4h}.$$

It is interesting to note that despite the fact that now the values from the $(n+1)$-th time level are present in (7), the scheme (2), (3) stays explicit. It is not necessary to compute the values H_j^* in the modified algorithm. The corrector step (3) is performed separately for H_j^{n+1} and $(Hu)_j^{n+1}$, i.e. at first, the values H_j^{n+1} are found from the continuity equation, and then the impulse $(Hu)_j^{n+1}$ is obtained by the explicit formula with using of the computed value H_j^{n+1} in the right-hand side (7) of the impulse equation.

Thus, contrary to [3], two equations are solved now on the predictor step, reducing significantly the computation time. In addition, all advantages of the original predictorcorrector scheme [3] remain when the right-hand side is computed by the formula (7). In particular, the preservation a state of rest on a fixed grid is kept valid.

Lemma 1 *If a nonuniform grid $\{x_j^n\}$ is fixed, and a fluid is at rest on the n-th time level*

$$\eta_j^n \equiv 0, \quad u_j^n \equiv 0, \tag{8}$$

then the predictor-corrector scheme (2), (3), (7) preserves a state of rest on the $(n+1)$-th time level.

Proof. From the condition (8) and the condition of grid immovability $x_t \equiv 0$ it follows that

$$\left(\bar{\Lambda}\vec{P} - \mathcal{L}\vec{G}\right)_{j+1/2}^{n} = 0,$$

therefore, on the predictor step

$$\hat{\vec{f}}_{j+1/2} = \frac{\vec{f}_j^n + \vec{f}_{j+1}^n}{2}.$$

Then from the formula (3) of the corrector step, with taking into account (7) and the equalities $h_j^{n+1} = h_j^n$ and $J_j^{n+1} = J_j^n$ for a fixed grid, it follows that $\eta_j^{n+1} \equiv 0$, $u_j^{n+1} \equiv 0$. Thus, a state of rest is preserved on the $(n+1)$-th time level.

3 NEW METHOD FOR SWITCHING SCHEMES

The formula (6) governs the switching from one scheme to another according to a local behavior of the vector $\vec{P} = \mathcal{L}\vec{u}_q$. For example, when the first of two conditions in (6) is satisfied in both neighboring points $q_{j-1/2}$ and $q_{j+1/2}$ and for both values $k = 1$ and $k = 2$, the computation of predictor values (2) is done with the identity matrix $\mathcal{D} = \mathcal{E}$, i.e. the scheme (2), (3) coincides locally (in the node q_j) with the Lax-Wendroff scheme on moving grid. The known or new schemes are obtained for other correlations between the components of the vector $\vec{P}$ in neighboring nodes. In particular, for

$$\theta_{j+1/2}^k = \theta_{0,j+1/2}^k, \quad \theta_{j-1/2}^k = \theta_{0,j-1/2}^k, \quad k = 1, 2, \tag{9}$$

the scheme (2), (3) in the node q_j turns into the upwind scheme of the first approximation order.

The switching from one scheme to another by the formula (6) is actually based on the behavior analysis of the derivative $\vec{u}_q$ of the solution vector, i.e. the derivatives H_q and $(Hu)_q$ of the full depth and full impulse. Considering that $H_q = \eta_q + h_q$, the behavior of the bottom function $h(x)$ can have a strong influence on the choice of a scheme when using this switching method. Nevertheless, relying on their long-term experience of numerical computations of movement of surface waves over irregular bottoms, the authors of the current work came to the conclusion that a switcher of schemes should analyze not the variation of the full depth H_q, but the variation of the free surface elevation η_q and also the velocity derivative u_q. In this new switching method all formulas remain the same, except for the expressions for $g^k_{j+1/2}$ where the components $\widetilde{p}^n_{k,j+1/2}$ of the new vector $\widetilde{\mathbf{P}}$, which do not contain the derivative h_q, are used instead of the components of the vector $\vec{P}$.

From the definition of the vector $\vec{P}$ it follows that

$$\vec{P}^n_{j+1/2} = (\mathcal{L}\vec{u}_q)^n_{j+1/2} = \frac{1}{(c^n_{j+1/2})^2} \begin{pmatrix} -c\eta_q + Hu_q \\ c\eta_q + Hu_q \end{pmatrix}^n_{j+1/2} + \left(\frac{h_q}{c}\right)^n_{j+1/2} \begin{pmatrix} -1 \\ 1 \end{pmatrix}.$$

Therefore, the vector $\vec{P}$ is represented as the sum of two vectors. One of these vectors depends on the behavior of the solution (the derivatives η_q, u_q), but is independent of the depth variation h_q. This first vector is taken as a new vector $\widetilde{\mathbf{P}}$.

4 CONSERVATIVE SCHEMES ON MOVING GRIDS FOR THE SHALLOW WATER EQUATIONS

It is known [6, 17] that the non-conservative schemes can diverge on discontinuous solutions, therefore, the conservation property is one of the important requirements to numerical schemes. For non-homogeneous systems of (1) type the conservation of a difference scheme means the satisfaction of the difference analogues of the balance equations, which express the variation laws for the so-called conservative variables. For the system of shallow water equations (1) the conservative variables are the full depth H and the full impulse Hu. The balance equations for these variables describe the mass conservation law and the full impulse variation law. For a case of a flat bottom the full impulse variation law turns into the conservation law.

When constructing the conservative schemes on moving grids, the formulas for grid node velocities must be consistent with the formulas for cell areas. The special approximation of these variables guarantees the satisfaction of the difference analogue of the geometric conservation law [18, 19], which is the necessary condition for consistency of the formulas. In [3, 18] an original procedure was suggested for constructing conservative schemes for the scalar conservation law. This procedure was based on a choice of the scheme parameter θ corresponding to a concrete scheme. The same approach can be used for the systems of equations as well.

For example, according to [18], in order to derive the upwind scheme on moving grids for the shallow water equations, it is sufficient to use the formulas (9) for the parameters $\theta^k_{j+1/2}$ in the conservative predictor-corrector scheme (2), (3). Let us provide the obtained conservative upwind scheme on moving grid in the equivalent divergent and non-divergent forms.

If the parameters θ^k, given by the equalities (9), are used in the scheme predictor-corrector (2), (3), then

$$\mathcal{D}\bar{\Lambda} = \frac{hJ}{\tau}\mathcal{S}, \quad \mathcal{D}\bar{\Lambda}^2 = \frac{hJ}{\tau}\left(\bar{\Lambda}^+ - \bar{\Lambda}^-\right), \quad \mathcal{R}\mathcal{D}\bar{\Lambda}^2\mathcal{L} = \frac{hJ}{\tau}\left(\bar{\mathcal{A}}^+ - \bar{\mathcal{A}}^-\right), \quad \mathcal{R}\mathcal{D}\bar{\Lambda}\mathcal{L} = \frac{hJ}{\tau}\mathcal{R}\mathcal{S}\mathcal{L}$$

then the scheme turns into the upwind scheme in the divergent form:

$$\frac{(J\vec{u})_j^{n+1} - (J\vec{u})_j^n}{\tau} +$$

$$+\frac{1}{h}\Big[\Big(\frac{\vec{f}_{j+1}^n + \vec{f}_j^n}{2} - \frac{\left(\bar{\mathcal{A}}^+ - \bar{\mathcal{A}}^-\right)_{j+1/2}^n}{2}\left(\vec{u}_{j+1}^n - \vec{u}_j^n\right) - (x_t\vec{u})_{j+1/2}^n + \frac{h}{2}\left(\mathcal{RSL}\vec{G}\right)_{j+1/2}^n\Big) - \quad (10)$$

$$-\Big(\frac{\vec{f}_j^n + \vec{f}_{j-1}^n}{2} - \frac{\left(\bar{\mathcal{A}}^+ - \bar{\mathcal{A}}^-\right)_{j-1/2}^n}{2}\left(\vec{u}_j^n - \vec{u}_{j-1}^n\right) - (x_t\vec{u})_{j-1/2}^n + \frac{h}{2}\left(\mathcal{RSL}\vec{G}\right)_{j-1/2}^n\Big)\Big] = \vec{G}_j^*,$$

where the right-hand side is calculated using the formula (7),

$$\mathcal{D} = \frac{hJ}{\tau}\begin{pmatrix} 1/|\bar{\lambda}_1| & 0 \\ 0 & 1/|\bar{\lambda}_2| \end{pmatrix}, \quad \mathcal{S} = \begin{pmatrix} s_1 & 0 \\ 0 & s_2 \end{pmatrix}, \quad \bar{\Lambda}^{\pm} = \begin{pmatrix} \bar{\lambda}_1^{\pm} & 0 \\ 0 & \bar{\lambda}_2^{\pm} \end{pmatrix},$$

$$\bar{\lambda}_k^{\pm} = \frac{\bar{\lambda}_k \pm |\bar{\lambda}_k|}{2}, \quad \bar{\mathcal{A}}^{\pm} = \mathcal{R}\bar{\Lambda}^{\pm}\mathcal{L},$$

and the following equalities are satisfied:

$$\bar{\Lambda} = \bar{\Lambda}^+ + \bar{\Lambda}^-, \quad \bar{\mathcal{A}}^+ + \bar{\mathcal{A}}^- = \bar{\mathcal{A}} = A - x_t\mathcal{E}.$$

The indices n and $j + 1/2$ are omitted here in order to simplify the notation.

The left part of the conservative upwind scheme (10) is written in the divergent form. Using the equivalent transformations this scheme can be written in the non-divergent form, which is analogous to the form of upwind schemes for scalar equations. The following equality is used:

$$\vec{f}_{q,j+1/2}^n = \left(\mathcal{A}\vec{u}_q\right)_{j+1/2}^n,$$

which is satisfied for the matrix $\mathcal{A}$ given by the formula (4), and the identity

$$(x_t\vec{u})_{q,j}^n = (x_{tq}\vec{u})_j^n + \frac{1}{2}\left[(x_t\vec{u}_q)_{j+1/2}^n + (x_t\vec{u}_q)_{j-1/2}^n\right],$$

where

$$(x_t\vec{u})_{q,j}^n = \frac{(x_t\vec{u})_{j+1/2}^n - (x_t\vec{u})_{j-1/2}^n}{h}; \quad x_{tq,j}^n = \frac{x_{t,j+1/2}^n - x_{t,j-1/2}^n}{h}.$$

As a result, the difference equation (10) takes on the form

$$\frac{(J\vec{u})_j^{n+1} - (J\vec{u})_j^n}{\tau} + \frac{1}{2}\Big[\mathcal{A}\vec{u}_q - \left(\bar{\mathcal{A}}^+ - \bar{\mathcal{A}}^-\right)\vec{u}_q - x_t\vec{u}_q + \mathcal{RSL}\vec{G}\Big]_{j+1/2}^n +$$
$$+\frac{1}{2}\Big[\mathcal{A}\vec{u}_q + \left(\bar{\mathcal{A}}^+ - \bar{\mathcal{A}}^-\right)\vec{u}_q - x_t\vec{u}_q - \mathcal{RSL}\vec{G}\Big]_{j-1/2}^n - (x_{tq}\vec{u})_j^n = \vec{G}_j^*.$$

Further, using the equality $\mathcal{A} = \mathcal{A}^+ + \mathcal{A}^-$ and the geometric conservation law [18]

$$J_j^{n+1} = J_j^n + \tau x_{tq,j}^n, \quad (11)$$

the final form of the upwind scheme in the non-divergent form is obtained:

$$\frac{\vec{u}_j^{n+1}-\vec{u}_j^n}{\tau}+\frac{1}{J_j^{n+1}}\Big[\left(\mathcal{A}^+\vec{u}_q\right)_{j-1/2}^n+\left(\mathcal{A}^-\vec{u}_q\right)_{j+1/2}^n\Big]=$$

$$=\frac{1}{J_j^{n+1}}\Big[\vec{G}_j^*-\frac{1}{2}\Big(\left(\mathcal{RSL}\vec{G}\right)_{j+1/2}^n-\left(\mathcal{RSL}\vec{G}\right)_{j-1/2}^n\Big)\Big]. \tag{12}$$

The explicit upwind scheme (12) is implemented as follows. At first, the full depth H_j^{n+1} is obtained from the first equation of the system (12) in all grid nodes. Then, using new values H^{n+1} in the right-hand side of (7), the full impulse $(Hu)_j^{n+1}$ is calculated. This scheme is conservative and preserves a state of rest.

Lemma 2 *The upwind scheme (12) preserves a state of rest (8) on a fixed grid.*

Proof. The preservation of a state of rest $\eta_j^{n+1}\equiv 0,\ u_j^{n+1}\equiv 0$ on the $(n+1)$-th time level follows from the formula (12) with taking into account the conditions (8), the equalities $x_t\equiv 0$ and $h_j^{n+1}=h_j^n$ for a fixed grid, and the formula for the right-hand side (7).

5 TESTING OF SCHEMES ON EXACT SOLUTION OF SHALLOW WATER EQAUTIONS

Some properties, which are inherent to the numerical solutions of linearized systems or scalar nonlinear equations, can not be strictly proved for the difference equations approximating the system of nonlinear shallow water equations. Therefore, it is very important to investigate the scheme properties using numerical tests.

In numerical modelling of a wave run-up on a coast one of the most popular tests is the problem of a wave run-up on a plane slope adjacent to a horizontal bottom with a constant depth [20, 22]. An initial wave is positioned above the horizontal bottom, propagates over it in the direction of the plane slope and runs up on the slope. For reliable estimates of inundation zones not only the quality algorithms for the detection of waterfront movement are needed, but also the reliable numerical methods for modelling of the initial stage of a wave movement including a propagation over a flat bottom. Let us present the results of this modelling using the described methods on adaptive grids.

In the considered test problem it is assumed that a bottom is horizontal $h(x)\equiv h_0$ and the initial conditions are given for $t=0$:

$$\eta(x,0)=\eta_0(x),\quad u(x,0)=u_0(x). \tag{13}$$

The numerical solution is compared with the exact solution of the Cauchy problem (1), (13), which can be found in [5]. In the case of the nonlinear dispersive equations [23, 24] the problem with the exact solution in the form of a solitary wave propagating over a flat bottom is included into the list of imperative tests. Yet, the exact solution [5] of the non-dispersive shallow water equations is rarely used for testing the numerical algorithms. The authors assume that the reason is the insufficient description of the method for obtaining the exact solution in [5]. Therefore, another way to derive the formulas of the exact solution is presented now.

Let us write down the shallow water equations (1) in Riemann invariants [7]:

$$r_t+\frac{3r+s}{4}r_x=0,\quad s_t+\frac{r+3s}{4}s_x=0, \tag{14}$$

where

$$r = u - 2c; \quad s = u + 2c; \quad c = \sqrt{gH}; \quad H = \eta + h_0. \tag{15}$$

The solution of the equations (14) is sought in the form of the r-wave propagating from right to left [25], i.e. under the assumption that $s \equiv s_0 = \text{const}$. Assuming that a fluid at infinity is in a state of rest, it follows that $s_0 = 2\sqrt{gh_0} = 2c_0$. Therefore, the formula $u + 2c = s_0$ leads to the expression of the velocity in terms of the full depth:

$$u(x,t) = 2c_0 - 2\sqrt{gH(x,t)} = 2c_0 - 2\sqrt{g\left[\eta(x,t) + h_0\right]}, \tag{16}$$

$$u_0(x) = u(x,0) = 2c_0 - 2\sqrt{gH_0(x)} = 2c_0 - 2\sqrt{g\left[\eta_0(x) + h_0\right]}. \tag{17}$$

If a new dependent variable is introduced:

$$p = \frac{3r + s_0}{4}, \tag{18}$$

then the equation for the invariant r is transformed into the Hopf-equaiton $p_t + pp_x = 0$. The solution of the Cauchy problem for this equation is found using the characteristics method and given implicitly by the formula [25]

$$p(x,t) = p_0(x - pt), \tag{19}$$

where p_0 is the initial function,

$$p_0(x) = \frac{3r(x,0) + s_0}{4} = \frac{3\left(u_0(x) - 2\sqrt{gH_0(x)}\right) + 2c_0}{4} = 2c_0 - 3\sqrt{gH_0(x)}. \tag{20}$$

Therefore, from (19) it follows the value $p(x,t)$ is the root p of the equation

$$p = 2c_0 - 3\sqrt{g\left(h_0 + \eta_0(x - pt)\right)} \tag{21}$$

for the given x, t. The obtained p is used for computing the free surface elevation $\eta(x,t)$. Taking into account the equalities (15), (16), (18), it is obtained that

$$\eta(x,t) = \left(\frac{2c_0 - p(x,t)}{3\sqrt{g}}\right)^2 - h_0. \tag{22}$$

Thus, the exact solution of the equations (1) is found using the following algorithm. The initial elevation $\eta_0(x)$ in the form of a continuous function is given for $t = 0$. The initial velocity $u_0(x)$, which is consistent with the initial elevation, is calculated using the formula (17). The root of the equation (21) is found at the time moment t in the point x. The elevation $\eta(x,t)$ is obtained using the formula (22), then the velocity $u(x,t)$ is calculated using (16).

With the help of the described method of characteristics it is possible to find the exact solution either for all $t > 0$ or until a gradient catastrophe moment t_*. Let us consider the initial elevation in the form of a solitary wave with the length λ [20]:

$$\eta_0(x) = \begin{cases} \dfrac{a}{2}\left[1 + \cos\left(\dfrac{2\pi(x - x_w)}{\lambda}\right)\right], & |x - x_w| \le \lambda/2, \\ 0, & |x - x_w| > \lambda/2, \end{cases} \tag{23}$$

where x_w is the abscissa of the wave top at $t = 0$, a is the wave amplitude. For $0 < t < t_*$ the length of the wave, moving to the left with the velocity $-c_0$, and its amplitude stay constant and equal to the corresponding values of the initial wave (23). The profile of the propagating wave will be deformed with time so that its leading edge is steepening and the trailing edge is flattening. This happens because the characteristics $dx/dt = p_0(x)$, going out from the interval $[x_w - \lambda/2,\, x_w]$, form a convergent bundle, and from the interval $[x_w,\, x_w + \lambda/2]$ – the divergent bundle. Therefore, the solution includes a compression wave and a rarefaction wave, which propagates before a compression wave and leads to the gradient catastrophe.

Fig. 1, *a* shows the exact solution $y = \eta(x, t)$ at $t = 5$ s (thin solid line). The non-dimensional (obtained by the division by h_0) values of parameters, defining the initial wave, are taken as follows:

$$a = 0.2, \quad x_w = 30, \quad \lambda = 10, \quad h_0 = 1.$$

For these parameter values the gradient catastrophe occurs at $t_* \approx 5.57$ s, therefore, the leading edge becomes close to a vertical line at $t = 5$ s.

Let us note that the equation (21) has the unique solution p for $t < t_*$, because the function

$$f(p;\, x, t) = p + 3\sqrt{g\,(h_0 + \eta_0(x - pt))} - 2c_0 \tag{24}$$

is a monotonically increasing function of the variable p for all x and $t \in [0, t_*)$. Fig. 2 shows the function $f(p;\, x, t)$ for the fixed values $t = 5$ s and $x \in [0,\, L]$. Here $L = 40$ and the non-dimensional variable $\bar{p} = p/c_0$ is plotted along the axis Op. The solid line denotes the line of level $f = 0$. It is clear that the equation $f = 0$ has one root p for each fixed value of the variable x. Some method for solving the nonlinear equations can be used for finding this root. $[p_1,\, p_2]$ can be taken as the initial interval, which contains the root, where

$$p_1 = 2c_0 - 3\sqrt{g\,(h_0 + a)}, \quad p_2 = -c_0.$$

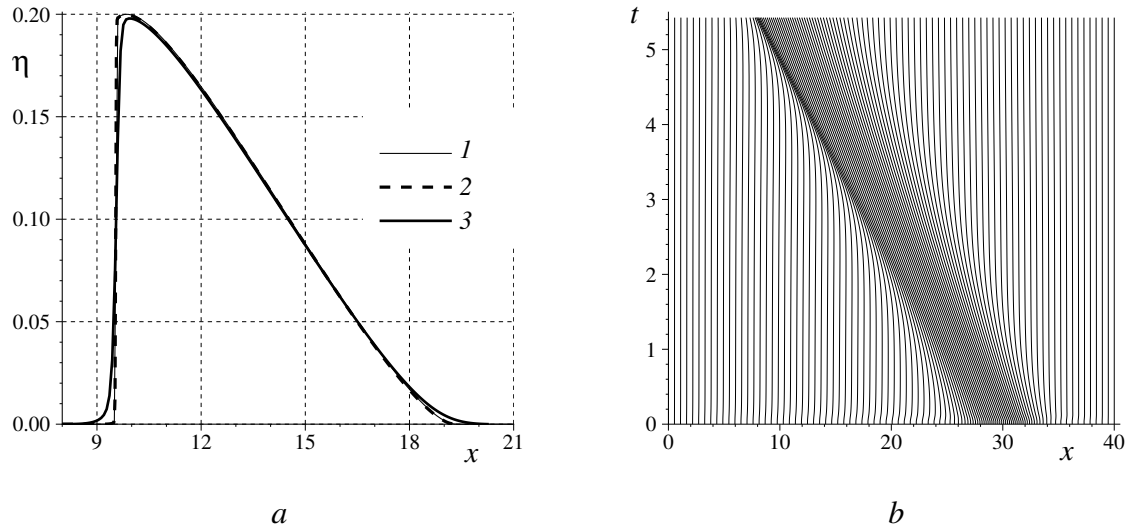

a *b*

Figure 1: Solitary wave (23) propagation over the horizontal bottom: *a* — exact solution (*1*) at $t = 5$ s and numerical solution, obtained using the predictor-corrector scheme (*2*) and the upwind scheme (*3*); *b* — the trajectories of the adaptive grid nodes

Fig. 1, *a* also shows the numerical solution, obtained using two schemes on adaptive grids on the interval $[0,\ L]$. The adaptive grids were constructed by the equidistribution method [18] with the control function

$$w^n_{j+1/2} = 1 + \alpha_0 \left|\eta^n_{j+1/2}\right| + \alpha_1 \frac{\left|\eta^n_{j+1} - \eta^n_j\right|}{x^n_{j+1} - x^n_j} \tag{25}$$

with the coefficient $\alpha_0 = 10$, $\alpha_1 = 10$. From Fig. 1, *b*, which presents the grid dynamics in the computation using the predictor-corrector scheme, it is seen that at $t = 0$ the nodes condense in the initial wave zone, then the continuous automatic redistribution of nodes occurs with time, and the condensation increases in the zone of the steepening leading wave edge. Such behavior of the adaptive grid increases the computational accuracy. Fig. 1, *a* shows that the exact solution and numerical solution, obtained by the predictor-corrector scheme, are visually indistinguishable, despite a rather small number of grid nodes ($N = 100$). The using of fixed uniform grids with the same number of nodes leads to a significant decrease of accuracy, being in good agreement with the conclusions of the works [3, 18, 19] where the solution of scalar equations on moving grids was considered.

Regarding to the upwind scheme, the using of adaptive grids also increases the accuracy in comparison with uniform grids, though not as much as for the predictor-corrector scheme (see Fig. 1, *a*, where the smearing of the wave borders and the decrease of its amplitude are seen for the upwind scheme).

6 ADAPTIVE GRID METHOD IN WAVE RUN-UP PROBLEMS

In [22] the adaptive grid method was used for the computation of the wave run-up in one-dimensional cross-sections drawn from some isobath to a chosen isobath on the dry land. The analytical solutions of the shallow water equations [20] were used for defining the waterfront point movement. These solutions were represented in the form of infinite series for one of possible cases of wave interaction with a coast and as the solution of the system of ordinary differential equations for two other cases. In the numerical computation [22] few first terms from the obtained series were used, and the Euler method of the second accuracy order was

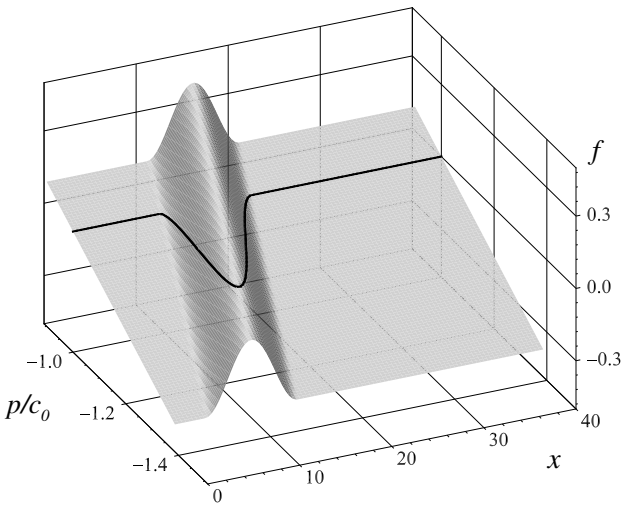

Figure 2: The function (24) at $t = 5$ s

used for the solution of the ordinary differential equations systems. In the present work, a larger number of terms in the partial sums of the series and a preciser methods for solving the ordinary differential equations are used.

6.1 Refined formulas for computing a waterfront point movement

Let us consider the wave run-up problem, where an unknown function $x = x_0(t)$, describing the law of the waterfront point movement, and the solution of the system of equations (1) for $x \geq x_0(t)$ are sought. Further, it is assumed that the initial data for the equations (1) are given not at $t = 0$, but at $t = t_0$, i.e. the initial position of the waterfront point $x_0(t_0) = x_{00}$ and the initial functions for $x \geq x_{00}$ are known

$$u(x, t_0) = u_0(x), \quad H(x, t_0) = H_0(x). \tag{26}$$

It is necessary to find $x = x_0(t)$, $u(x, t)$, $H(x, t)$ at $t > t_0$. The additional boundary condition in the waterfront point consists in the requirement that the full depth in this point is equal to zero at all time moments:

$$H(x_0(t), t) \equiv 0. \tag{27}$$

Depending on the initial data (26) three regimes are possible for wave interaction with a coast [20]. The first case is the run-up of a non-breaking wave on a coast:

$$H_x \mid_{x=x_0(t)} \neq 0. \tag{28}$$

Let us show that for the velocity of the waterfront point movement $U(t) = u(x_0(t), t)$ the equality:

$$U(t) = \dot{x}_0(t), \quad t \geq t_0. \tag{29}$$

is satisfied. Here and further a dot above is used to denote a time derivative of a function which depends on one variable t only. Let us introduce a new independent variable $\xi = x - x_0(t)$ and write down the system (1) in new coordinates (ξ, t):

$$\tilde{H}_t + (\tilde{u} - \dot{x}_0)\tilde{H}_\xi + \tilde{H}\tilde{u}_\xi = 0, \quad \tilde{u}_t + (\tilde{u} - \dot{x}_0)\tilde{u}_\xi + g\tilde{H}_\xi = g\tilde{h}_\xi, \quad \xi \geq 0, \tag{30}$$

where

$$h(x) = h\left(x(\xi, t)\right) = \tilde{h}(\xi, t),\ H(x, t) = H(x(\xi, t), t) = \tilde{H}(\xi, t),\ u(x, t) = u(x(\xi, t), t) = \tilde{u}(\xi, t).$$

The waterfront point is immovable in new variables (ξ, t) and it has the same coordinate $\xi = 0$ for all $t \geq t_0$, and here

$$\tilde{H}(0, t) \equiv 0. \tag{31}$$

Using the identity (31) in the first equation of the system (30) for $\xi = 0$, the identity's corollary $\tilde{H}_t(0, t) = 0$ and the condition (28), it is obtained that $\dot{x}_0 - \tilde{u}|_{\xi=0} = 0$, which coincides with the equality (29).

The law of movement of the waterfront point is sought in the form of the power series in time

$$x_0(t) = x_{00} + x_{01}(t - t_0) + x_{02}\frac{(t - t_0)^2}{2} + x_{03}\frac{(t - t_0)^3}{6} + x_{04}\frac{(t - t_0)^4}{24} + O\left((t - t_0)^5\right). \tag{32}$$

From the equality (29) it follows that

$$U(t) = \dot{x}_0(t) = x_{01} + x_{02}(t-t_0) + x_{03}\frac{(t-t_0)^2}{2} + x_{04}\frac{(t-t_0)^3}{6} + O\left((t-t_0)^4\right), \qquad (33)$$

i.e. $x_{01} = U(t_0) = u_0(x_0(t_0)) = u_0(x_{00}) = u_{00}$, where u_{00} denotes the fluid velocity in the waterfront point at the initial time moment.

The recursive formulas [20] can be used to find other coefficients. However, it is not convenient for the numerical realization of the algorithm, because one and the same term of the series has to be approximated with a different order, depending on how many terms are taken in the partial sum for using in the difference boundary condition. A more preferable approach is to use the explicit formulas for computing the coefficients x_{0k} ($k \geq 2$) in terms of the initial data of the problem.

In order to calculate the coefficient x_{02}, the second equation of the system (30) is considered for $\xi = 0$ and $t = t_0$: $\dot{U}(t_0) = -g\eta_0'(x_{00})$. On the other hand, from (33) it follows that $\dot{U}(t_0) = x_{02}$, therefore

$$x_{02} = -g\eta_0'(x_{00}). \qquad (34)$$

Here and further a prime denotes a space derivative of a function which depends on one variable x only.

For finding x_{03} the equations, obtained as the result of the differentiation of the first equation of the system (30) with respect to the variable ξ, and the second equation — with respect to the variable t:

$$\begin{aligned} \tilde{H}_{\xi t} + (\tilde{u} - \dot{x}_0)\tilde{H}_{\xi\xi} + 2\tilde{H}_\xi\tilde{u}_\xi + \tilde{H}\tilde{u}_{\xi\xi} = 0, \\ \tilde{u}_{tt} + (\tilde{u}_t - \ddot{x}_0)\tilde{u}_\xi + (\tilde{u} - \dot{x}_0)\tilde{u}_{\xi t} + g\tilde{H}_{\xi t} = g\dot{x}_0 h''. \end{aligned} \qquad (35)$$

Taking $\xi = 0$ in these equations and then taking $t = t_0$, the formula

$$x_{03} = \ddot{U}(t_0) = g\left(2u_0'H_0' + u_{00}h''\right)\Big|_{x=x_{00}} \qquad (36)$$

is derived.

The coefficient x_{04} is computed using the equations (30), (36), and the following equations, which are obtained from them by the differentiation with respect to the variables t and ξ:

$$\begin{aligned} &\tilde{H}_{\xi tt} + (\tilde{u}_t - \ddot{x}_0)\tilde{H}_{\xi\xi} + (\tilde{u} - \dot{x}_0)\tilde{H}_{\xi\xi t} + 2\tilde{H}_{\xi t}\tilde{u}_\xi + 2\tilde{H}_\xi\tilde{u}_{\xi t} + \tilde{H}_t\tilde{u}_{\xi\xi} + \tilde{H}\tilde{u}_{\xi\xi t} = 0, \\ &\tilde{u}_{ttt} + (\tilde{u}_{tt} - \dddot{x}_0)\tilde{u}_\xi + 2(\tilde{u}_t - \ddot{x}_0)\tilde{u}_{\xi t} + (\tilde{u} - \dot{x}_0)\tilde{u}_{\xi tt} + g\tilde{H}_{\xi tt} = g\left[\ddot{x}_0 h'' + (\dot{x}_0)^2 h'''\right], \\ &\tilde{u}_{\xi t} + (\tilde{u}_\xi)^2 + (\tilde{u} - \dot{x}_0)\tilde{u}_{\xi\xi} + g\tilde{H}_{\xi\xi} = gh''. \end{aligned} \qquad (37)$$

If $\xi = 0$ is taken in these equations, and the equalities (29), (31) and their corollary $\dot{U}(t) = \ddot{x}_0(t)$, $\ddot{U}(t) = \dddot{x}_0(t)$, $\tilde{H}_t(0,t) = 0$ are taken into account, then the system of equations in the point $\xi = 0$ is obtained:

$$\begin{gathered} \tilde{H}_{\xi tt} + 2\tilde{H}_{\xi t}\tilde{u}_\xi + 2\tilde{H}_\xi\tilde{u}_{\xi t} = 0, \quad \tilde{H}_{\xi t} + 2\tilde{H}_\xi\tilde{u}_\xi = 0, \quad \tilde{u}_{\xi t} + (\tilde{u}_\xi)^2 + g\tilde{H}_{\xi\xi} = gh'', \\ \ddot{U} + g\tilde{H}_{\xi tt} = g\left[\ddot{x}_0 h'' + (\dot{x}_0)^2 h'''\right]. \end{gathered}$$

If the value $\tilde{H}_{\xi tt}$ is eliminated from the last equation using the first three equations, and $t = t_0$ is set, then the expression is obtained for the coefficient x_{04} in terms of the initial data:

$$x_{04} = \ddot{U}(t_0) = g\Big[u_{00}^2 h''' - \eta_0' h'' - 2H_0' \left(g\eta_0'' + 3(u_0')^2\right)\Big]\Big|_{x=x_{00}}. \tag{38}$$

If at the time moment $t = t_0$ the condition (28) is not satisfied, then two situations are possible: either $H_x(x_{00}, t_0) = 0$ or $H_x(x_{00}, t_0) = \infty$. The first case corresponds to a non-breaking wave run-up, for which the tangential line to free surface at the waterfront point coincides at $t = t_0$ with the tangential line to the bottom surface. The second case corresponds to a breaking wave run-up. In both cases the motion law for the waterfront point is defined as the solution of the system of ordinary differential equation [20]

$$\dot{x}_0 = U(t), \quad \dot{U} = gh'(x_0(t)) \tag{39}$$

with the initial conditions

$$x_0(t_0) = x_{00}, \quad U(t_0) = u_*, \tag{40}$$

here $u_* = u_{00}$ for a wave with tangency and $u_* = u_{00} - 2\sqrt{gH_{00}}$ for a breaking wave.

6.2 Computational algorithm

For the numerical solution of the wave run-up problem the above predictor-corrector scheme on adaptive grid $\left\{x_j^n\right\}$ $(j = 0, \ldots, N)$ is used. At every time level the left nodes x_0^n coincides with the moving waterfront point $x_0(t^n)$. It is assumed that the velocity, the full depth, and the position of the waterfront point are known at the time level $t = t^n$, and it is required to find these values on the next time level $t^{n+1} = t^n + \tau$.

In order to use the predictor-corrector scheme for computing the free surface elevation η_j^{n+1} and the velocity u_j^{n+1}, it is first necessary to generate the grid $\left\{x_j^{n+1}\right\}$. Therefore, a new position of the waterfront point, i.e. the far left node x_0^{n+1}, has to be known. The right boundary is assumed to be fixed, therefore, $x_N^{n+1} = L$. The difference non-reflecting boundary condition [22] is given in this node and used to obtain the values η_N^{n+1} and u_N^{n+1}.

In the non-degenerate case (28), the difference analogues of the partial sums of the series (32) and (33) are used to compute the coordinate x_0^{n+1} and the velocity u_0^{n+1}:

$$x_0^{n+1} = x_0^n + u_0^n\tau + x_{02}\frac{\tau^2}{2} + x_{03}\frac{\tau^3}{6} + x_{04}\frac{\tau^4}{24}, \quad u_0^{n+1} = u_0^n + x_{02}\tau + x_{03}\frac{\tau^2}{2} + x_{04}\frac{\tau^3}{6}. \tag{41}$$

The difference formulas for the coefficients x_{0k} $(k = 2, 3, 4)$ are obtained as the result of the approximation of the derivatives from the right-hand sides of the equalities (34), (36), (38) using the one-sided differences of corresponding order in the left node x_0^n of the non-uniform grid.

The first formula (41) shows that in order to calculate the position of the waterfront point x_0^{n+1} with the accuracy order $O(\tau^5)$ it is sufficient to approximate the coefficient x_{02} with the error $O(h^3)$, the coefficient x_{03} — with $O(h^2)$, and x_{04} — with $O(h^1)$. Here it is assumed that the law of passage to the limit has the form æ = const. Therefore, in the formula for the coefficient

$$x_{02} = -g\frac{\eta_{q,0}^n}{x_{q,0}^n} \tag{42}$$

the finite differences of the third order are used

$$\eta^n_{q,0} = \frac{-11\eta^n_0 + 18\eta^n_1 - 9\eta^n_2 + 2\eta^n_3}{3h}, \quad x^n_{q,0} = \frac{-11x^n_0 + 18x^n_1 - 9x^n_2 + 2x^n_3}{3h}.$$

As in [18], it is assumed that the nodes x^n_j of a non-uniform moving grid are the images of the nodes $q_j \in [0,\, 1]$ of a uniform fixed grid with the step $h = 1/N$ under some coordinate mapping $x = x(q,t)$. At each time moment t the mapping transforms in one-to-one manner the interval $[0,\, 1]$ to $[x_0(t),\, L]$. Using the transformation $x = x(q,t)$ the derivatives with respect to x can be expressed in terms of the derivatives with respect to q, as for instance $\eta_x = \eta_q/x_q$. On the discrete level it means that the problem of the approximation of the derivatives on a non-uniform moving grid x^n_j can be replaced by a simpler problem of their approximation of a uniform fixed grid q_j. This is used in the formula (42) according to which the approximation formula for the coefficient (36) has the following form:

$$x_{03} = g\frac{1}{(x^n_{q,0})^2}\left[2u^n_{q,0}H^n_{q,0} + u^n_0\left(h^n_{qq,0} - h^n_{q,0}\frac{x^n_{qq,0}}{x^n_{q,0}}\right)\right]. \tag{43}$$

As it was stated above, it is sufficient to approximate the derivatives entering into this formula by the one-sided differences of the second order:

$$u^n_{q,0} = \frac{-3u^n_0 + 4u^n_1 - u^n_2}{2h}, \quad H^n_{q,0} = \frac{-3H^n_0 + 4H^n_1 - H^n_2}{2h}, \quad x^n_{q,0} = \frac{-3x^n_0 + 4x^n_1 - x^n_2}{2h},$$

$$h^n_{qq,0} = \frac{2h^n_0 - 5h^n_1 + 4h^n_2 - h^n_3}{h^2}, \quad x^n_{qq,0} = \frac{2x^n_0 - 5x^n_1 + 4x^n_2 - x^n_3}{h^2}.$$

As far as the derivatives from the formula (38) have to be calculated with the first order only, it is easier to write down the approximation formula for x_{04} immediately on a non-uniform grid $\{x^n_j\}$:

$$x_{04} = g\Big[(u^n_0)^2 h^n_{xxx,0} - \eta^n_{x,0}h^n_{xx,0} - 2H^n_{x,0}\left(g\eta^n_{xx,0} + 3(u^n_{x,0})^2\right)\Big], \tag{44}$$

where the following formulas are used for the first difference derivatives:

$$H^n_{x,0} = \frac{H^n_1 - H^n_0}{x^n_1 - x^n_0}, \tag{45}$$

and the known formulas [17] of the first order on a non-uniform grid are used for the second and third difference derivatives.

For a plane slope

$$z = -h(x) = \begin{cases} z_0 - x\,\mathrm{tg}\,\theta & \text{for} \quad 0 \le x \le x_s, \\ -1 & \text{for} \quad x_s \le x \le L, \end{cases} \tag{46}$$

adjacent to a horizontal bottom of a constant depth h_0, the obtained formulas significantly simplify, because $h' = \mathrm{tg}\theta$, $h'' = h''' = 0$. In the formula (46) $\theta > 0$ is the slope angle, $z_0 > 0$ is the height of the "dry land" in the point $x = 0$, $x_s = (z_0 + 1)\mathrm{ctg}\,\theta$ is the abscissa of the slope bed. The value of z_0 is adjusted so that the maximal wave run-up on a coast does not exceed this value.

As it was shown above, for the second and third regimes of wave interaction with a coast, the motion law of the waterfront point is defined as the solution of the system of two ordinary differential equations (39). The Euler method was used to solve this system in [20]. In the present work the Runge-Kutta method of the fourth accuracy order is used with the initial conditions $x_0(t^n) = x_0^n$, $U(t^n) = u_*$ for the second regime, and $u_* = u_1^n - 2\sqrt{gH_1^n}$ – for the third one.

In the case of a plane slope (46) the system (39) has the exact analytical solution

$$x_0^{n+1} = x_0^n + \tau u_* + \frac{\tau^2}{2} g \,\mathrm{tg}\theta, \quad u_0^{n+1} = u_* + \tau g \,\mathrm{tg}\theta \tag{47}$$

and both methods (Euler and Runge-Kutta) give the same results.

As in [22], in numerical computation a concrete regime of wave interaction with a coast is defined according to the value of the difference derivative $H_{x,0}^n$ in the node x_0^n of a moving grid. In [22] this derivative was calculated with the help of the one-sided difference of the first order (45). In the present work the formula of the second order

$$H_{x,0}^n = \frac{-3H_0^n + 4H_1^n - H_2^n}{-3x_0^n + 4x_1^n - x_2^n}$$

is used. If this difference derivative satisfies the condition $m \le \left|H_{x,0}^n\right| \le M$, where m, M are the given numbers ($0 < m \ll M$), then it is assumed that the first regime is realized, and for the condition $\left|H_{x,0}^n\right| < m$ – the second regime. The inequality $\left|H_{x,0}^n\right| > M$ is used as the criteria for the third regime.

The above formulas for the position of a moving waterfront point x_0^{n+1} and its velocity u_0^{n+1} depend on a regime of wave interaction with a coast, whereas the full depth in the far left grid node is equal to zero $H_0^{n+1} = 0$ for all regimes.

Lemma 3 *If the position of the waterfront point and its velocity are defined by the formulas (41)–(44), then the predictor-corrector scheme (2), (3), (7) preserves a state of rest (8).*

Proof. Under the rest condition (8) the first regime of wave interaction with a coast is realized ($m \le \left|H_{x,0}^n\right| \le M$). It is easy to check that with the use of the formulas (41)–(44) the waterfront point has a zero velocity ($u_0^{n+1} = 0$) and the same position ($x_0^{n+1} = x_0^n$) at the time moment t^{n+1}. Then, from the boundary condition $H_0^{n+1} = 0$ it follows that the free surface elevation does not change in this point: $\eta_0^{n+1} = \eta_0^n = 0$. Further, the proof is the same as in the lemma 1.

6.3 Some numerical results of modelling of a solitary wave run-up on a plane slope

Let us consider the results of the numerical solution of the problem on a solitary wave run-up on a plane slope. A solitary wave is given at the initial time moment $t = 0$:

$$\eta_0(x) = a_0 \mathrm{ch}^{-2}\left(\frac{\sqrt{3a_0 g}}{2U_0}(x - x_w)\right), \quad H_0(x) = h(x) + \eta_0(x), \quad u_0(x) = -U_0 \frac{\eta_0(x)}{H_0(x)}, \tag{48}$$

where a_0 is the amplitude of the wave, $x = x_w$ is the abscissa of the wave top, $U_0 = \sqrt{g(h_0 + a_0)}$, $x \in [0,\, L]$. A plane slope is given by the formula (46) with the value $z_0 = 1$.

At the initial time moment the wave top (48) was well spaced from the slope bed x_s and from the right boundary $x = L$. This guaranteed the position of the wave main part above the horizontal part of the bottom and the independence of the run-up picture on the boundary conditions on the right boundary up to some time moment. As the computations have shown,

the wave can break in a long-continued propagation above a horizontal bottom. Thus, if the interaction of a non-deformed solitary wave with a slope has to be investigated in the framework of the shallow water model, then a wave should not be initially positioned too far from a slope.

For a small amplitude a_0 (for instance, $a_0 = 0.01$) the initial solitary wave has a larger effective length, therefore, the following values of the top abscissa of the initial wave and the right boundary were chosen in the numerical experiments:

$$x_w = x_s + 30, \quad L = x_w + 30.$$

For shorter waves (for instance, $a_0 = 0.1$) the point $x = x_w$ was positioned closer to the slope and the domain length was smaller:

$$x_w = x_s + 20, \quad L = x_w + 20.$$

Fig. 3 shows the maximal wave amplification (the maximal wave run-up on a plane slope taken relative to the amplitude a_0 of the initial wave). The markers *1* correspond to the refined formulas for computing the waterfront point movement, derived in the present work. The markers *4* are obtained when using the formulas from [20, 22], i.e. the first three terms in the partial sums (41). For the small amplitude a_0 the results are nearly the same (Fig. 3, *a*). For the initial amplitude, increased ten times, the difference becomes visible, especially for small slope angles (Fig. 3, *b*). The computations with other wave amplitudes have proved the conclusion that for small slope angles and large values a_0 the refined formulas gave the results which differ from those obtained by the previous formulas.

In many works, devoted to the investigation of a wave run-up on a coast, the comparison is done with the values obtained by the analytical formula [21]

$$\frac{R}{a_0} = 2.831\sqrt{\operatorname{ctg}\theta}\left(\frac{a_0}{h_0}\right)^{1/4}. \tag{49}$$

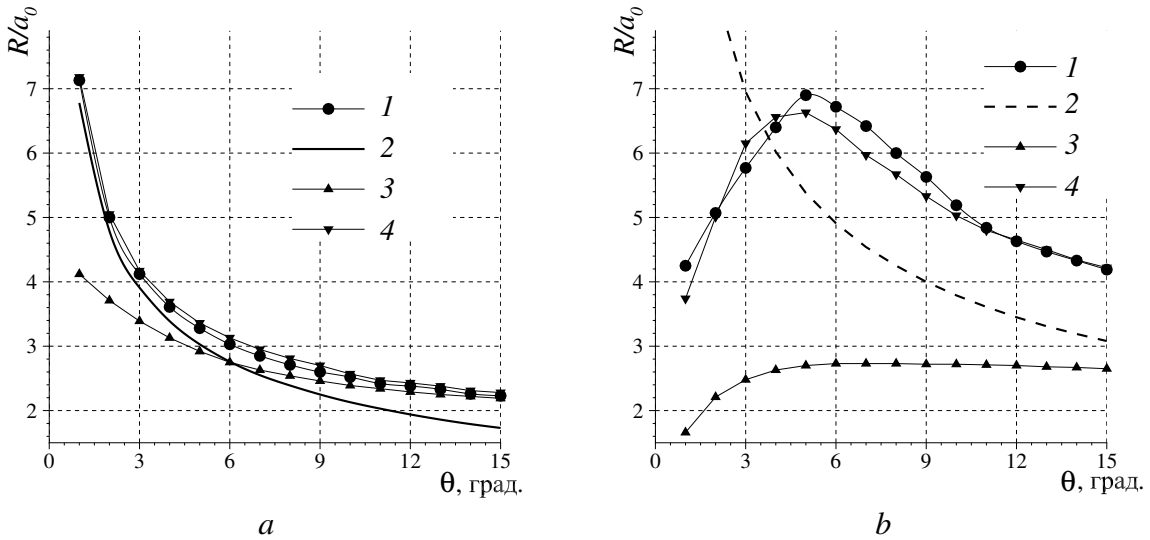

Figure 3: The maximal wave amplification with respect to a slope angle: $a_0/h_0 = 0.01$ (*a*), 0.1 (*b*). *1* (the refined formulas for the waterfront point movement,) *4* (the formulas from [20, 22]) — the numerical computation for the plane slope; *2* — the analytical dependency (49); *3* — the numerical computation for the vertical wall, positioned at the depth $h_{\text{wall}} = a_0$

However, this formula has to be used carefully, because it has a very narrow domain of applicability. According to [21, 26] the following restrictions are the conditions of applicability:

$$\frac{a_0}{h_0} \gg (0.288 \operatorname{tg}\theta)^2, \tag{50}$$

$$\frac{a_0}{h_0} < 0.479(\operatorname{tg}\theta)^{10/9}. \tag{51}$$

Fig. 3 shows the values (lines *2*) of the maximal wave amplification obtained by the formula (49). If it is held that the lower boundary of the applicability domain is defined by the expression in the right-hand side of the inequality (50), then nearly the whole line *2* in Fig. 3, *a* (except for the small upper part corresponding to angles in the vicinity $\theta = 1^\circ$) lies in the domain of applicability.

It is known that the value of the maximal amplification R/a_0 for a solitary wave run-up on a vertical wall is greater than two [27], and on a plane slope – greater than on a vertical wall [14]. However, for the angles greater than 11° the formula (49) gives the value less than two (Fig. 3, *a*, line *2*), i.e. even less than for the run-up on the vertical wall (markers *3*). This causes doubts in the physical consistency of the formula for $a_0/h_0 = 0.01$ and $\theta > 11^\circ$. Thus, the analytical formula (49) is applicable only for small angles θ and, therefore, in the restriction (50) the sign $\gg$ means that the expression in the right-hands side must be significantly smaller than the expression on the left. Hence, even for such small initial amplitude of a running wave it is possible to compare with the analytical formula only for this small range of angles θ, and the range can not be determined by the equality (50).

If this range exists, then Fig. 3, *b* shows that the refined formulas for the waterfront point movement (markers *1*) give the numerical run-up values which are slightly closer to analytical ones than those obtained by the formulas from [20, 22] (markers *4*). For the amplitude $a_0/h_0 = 0.1$ the analytical formula (49) is not applicable because of the restrictions (50), (51). Therefore, it makes no sense to use it for the comparison with numerical results. In order to emphasize this fact, the analytical dependency (49) is shown in Fig. 3, *b* by the dash line *2*.

The interesting peculiarity of the dependency of the maximal wave amplification R/a_0 on the angle θ is its non-monotonic character for large amplitudes (markers *1* in Fig. 3, *b*). The reason for the non-monotonicity is the wave breaking on the plane slope. Fig. 4, *a* shows the wave run-up on a plane slope and the subsequent run-down. Let us note, that the wave with negative polarity and significant amplitude is generated near the initial waterfront point position after the main run-down. This wave produces the whole series of run-ups and run-downs with damping amplitudes, that is physically explainable but has not been noted in the previous publications on the subject. The same figure shows that the leading edge of the initial wave is steepening when approaching to the waterfront point.

For the detailed investigation of this stage of run-up processes, Fig. 4, *b* shows the free surface elevation profiles at the initial time moment, wave breaking moment, and run-up start moment. By the moment of breaking the wave amplitude (line *2*) has become greater than the initial one (line *1*), and its leading edge has become nearly vertical. Here the wave has not yet reached the initial waterfront point position (left circle on the axis Ox), and the wave top has made the way slightly greater than one third of the slope length, counting from the starting point of the slope (right circle on the axis Ox).

After the wave breaking moment the wave amplitude and velocity decrease, and the wave actually approaches the waterfront point with a significantly smaller height than before the

breaking moment and, in this case, even smaller than the initial height a_0 (line *3*). This causes the fact that for small slope angles θ the run-up can be smaller than for larger angles. Let us note that this does not occur for small initial amplitudes a_0. Here the wave is very long, has low gradient slopes, and is not able to break even for small slope angles θ, i.e. on the long slope.

Let us also note that for the considered amplitude $a_0/h_0 = 0.1$ the wave breaking on the flat slope occurs for the slope angle $\theta_* \approx 6^\circ$. The formula (51) gives the threshold value $\theta_* \approx 12^\circ$. There exist other theories which provide another criteria for breaking and another threshold values accordingly. In the considered case the deviation of threshold values in numerical and analytical computations can be explained by the fact that the already deformed wave, with a steeper leading edge which is greater than that one of the initial wave (48), actually reaches the slope.

In many works, where the real problems are solved, the modelling is done for a run-up not on a coast but on a vertical wall positioned on a coast line. This significantly simplifies the computational algorithm, but leads to the errors in computations of the maximal wave amplification and, consequently, to the errors in the definition of inundation zones.

In one-dimensional case, a coast is substituted by a vertical wall in the initial position of the waterfront point $x_{00} = z_0 \mathrm{ctg}\theta$, and the impermeability condition $u(x_{00}, t) = 0$ is set meaning that the mobility of the waterfront point is ignored. The bottom (46) in the vicinity of the wall is modified so that if the depth becomes less than some given value h_{wall}, then it is assumed that $h(x) = h_{\text{wall}}$. In other words, the bottom in the vicinity of the wall becomes horizontal with the depth h_{wall}, i.e. the bottom is "cut" and straighten in the vicinity of the point x_{00}. If the depth is greater than h_{wall}, then the bottom form does not change.

Multiple computations were done for the problem on a wave run-up on a vertical wall. Some results are presented in Fig. 3 (markers *3*). It is seen that, as in the case of a wave run-up on a coast, the dependency of the maximal wave amplification R/a_0 on bottom slope angles has monotonic character for small amplitudes and non-monotonic – for large ones. In the last case the reason is still the breaking of the wave on the slope even before approaching the vertical

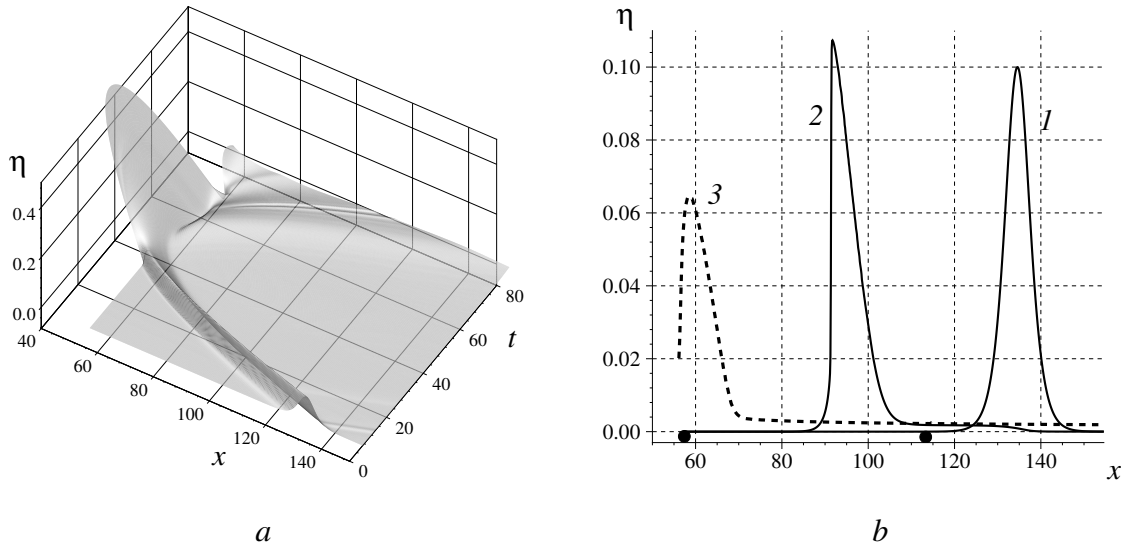

Figure 4: The run-up of the solitary wave (48) with the amplitude $a_0/h_0 = 0.1$ on the plane slope with the slope angle $\theta = 1^\circ$: *a* — the free surface elevation $z = \eta(x, t)$; *b* — the free surface elevation $\eta(x, t)$ at the initial time moment $t = 0$ (*1*), at the wave breaking moment $t = 12.64$ s (*2*), at the run-up start moment $t = 29.97$ s (*3*)

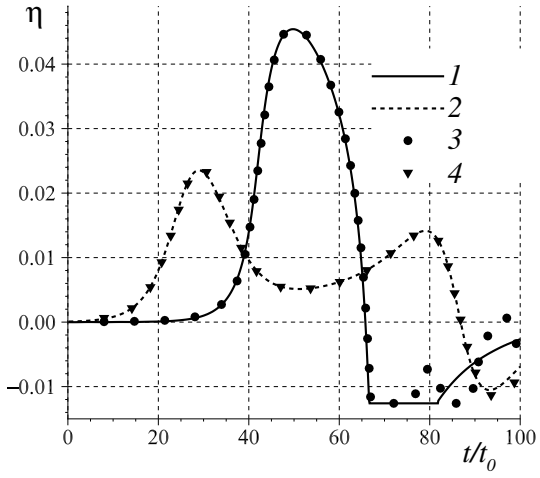

Figure 5: The mareograms, obtained analytically (lines) and numerically (markers) in the points, positioned to the right of the initial position of the waterfront point at the distances 0.25 (*1, 3*) and 9.95 (*2, 4*)

wall. For small amplitudes and large slope angles the values of the maximal wave amplification are practically indistinguishable for the run-up on the wall and for the run-up on the coast, but for large amplitudes they differ even for large slope angles. The greatest difference is observed for $\theta \approx 6^\circ$ (see Fig. 3, *b*). Here the run-up on the coast is significantly larger than on the vertical wall.

By now, a large set of test problems [28] has been formed, which are imperative for validation check of the results obtained by the numerical algorithms and for comparison of the characteristics of different algorithms [29]. One of these tests specifies the comparison of numerical results with the analytical solution of the problem on the run-up of the solitary wave with the small amplitude $a_0/h_0 = 0.019$ on the low gradient plane slope (46) with the slope angle $\theta = \arctan(1/19.85) \approx 2.88^\circ$.

Fig. 5 presents the mareograms, recorede by two virtual mareographs positioned at the distances 0.25 and 9.95 to the right of the initial position of the waterfront point x_{00}. For the first mareograph ($x = x_{00} + 0.25$), positioned near the initial waterfront point, there exist a time interval when the bottom drying occurs. The figure depicts this fact by the horizontal line drawn on the height $\eta \approx -0.012594$. In the position of the second mareograph ($x = x_{00} + 9.95$) the bottom drying does not occur. Figure shows that the numerical results, obtained using the predictor-corrector scheme, are visually indistinguishable from the analytical solution in the run-up phase and in the major part of the run-down phase. The difference can be seen only in the time interval from $t = 75$ to $t = 100$, where t is the non-dimensional time obtained by the division of the dimensional time by the value $t_0 = \sqrt{g/h_0}$. This difference can be attributed to the fact that the analytical formula for the exact solution, which was derived for non-breaking waves, becomes incorrect on this time interval because of the wave breaking at the end of the run-down phase. In fact, according to the conclusions in [26], if the condition (51) is fulfilled, then the wave does not break in the run-down phase. But in the considered case this condition is violated, because $a_0/h_0 = 0.019$ and the right-hand side of the inequality (51) takes the value equal to 0.0173.

7 CONCLUSIONS

An improved adaptive grid method is considered for the numerical solution of the problems on propagation and run-up of surface waves, described by the one-dimensional shallow water model. The modified algorithm for the realization of the explicit predictor-corrector scheme is presented, which is based on the new way of computation of the right-hand side of the shallow water equations on irregular bottom. The algorithm provides savings in computational time in comparison with its earlier version [3] while preserving the approximation order. Also the algorithm guarantees the preservation of the state of rest in transition from one time level to a next one. A new method for choosing the scheme parameters on the basis of the analysis of the differential approximation is suggested that guarantees the satisfaction of the TVD-property for the improved predictor-corrector scheme. The presented method for construction of different conservative schemes on moving grids is based on an appropriate choice of the scheme parameters for the predictor–corrector scheme, which represents the canonical form of the two-layer explicit schemes for the shallow water equations. As an example, a conservative upwind scheme on moving grid is provided in the divergent and non-divergent forms. The properties of the upwind scheme and the predictor–corrector scheme on dynamically adaptive grids are demonstrated for the exact solution of the nonlinear shallow water equations

Using the known analytical solutions of the shallow water equations in the vicinity of the water-land boundary the improved difference boundary conditions are obtained at the moving waterfront point. These boundary conditions approximate the analytical solutions with a higher accuracy than the conditions used earlier [20]. It is proved that if a fluid is at rest and has a non-perturbed free boundary at the initial time moment, then the difference predictor-corrector scheme on adaptive grid preserves the state of rest at all subsequent time moments when the newly obtained conditions are used. This is one of the advantages of the developed boundary conditions in comparison with the known shock-capturing methods, where the preservation of the state of rest is usually problematic for the run-up problems. The numerical experiments have shown that for the run-up problems the substitution of a slope by a vertical wall in the initial position of the waterfront point leads to the significant change of the wave amplification in the case of very smooth slopes even if a wall embedding is small.

The obtained results will find the application in the solution of two-dimensional problems in the framework of the shallow water model and in the algorithms for solution of the nonlinear dispersive equations [23, 24].

Funding: the work was supported by the Russian Scientific Foundation (project No. 14-17-00219).

REFERENCES

[1] Yu.I. Shokin, Z.I. Fedotova, G.S. Khakimzyanov, Hierarchy of nonlinear models of the hydrodynamics of long surface waves. *Doklady Physics*, **60(5)**, 168–172, 2015.

[2] E. Toro, P. García-Navarro, Godunov-type methods for free-surface shallow flows: A review. *Journal of Hydraulic Research*, **45(6)**, 736–751, 2007.

[3] G.S. Khakimzyanov, N.Yu. Shokina, Adaptive grid method for one-dimensional shallow water equations. *Computational Technologies*, **18(3)**, 54–79, 2013. (in Russ.)

[4] M.E. Vazquez-Cendon, Improved treatment of source terms in upwind schemes for the shallow water equations in channels with irregular geometry. *Journal of Computational Physics*, **148(2)**, 497–526, 1999.

[5] N.E. Voltsinger, E.N. Pelinovskii, K.A. Klevannyi, *The long-wave dynamics of the coastal zone*. Leningrad: Gidrometeoizdat, 1989. (in Russ.)

[6] R.J. LeVeque, *numerical methods for conservation laws*. Berlin: Birkhäuser Verlag, 1992.

[7] E.F. Toro, *Riemann solvers and numerical methods for fluid dynamics: a practical introduction*. Berlin: Springer-Verlag, Springer-Verlag, 2009.

[8] Lynch D.R. Gray W.G., Finite element simulation of flow in deforming regions. *Journal of Computational Physics*, **36**, 135–153, 1980.

[9] J. Hou, Q. Liang, H. Zhang, R. Hinkelmann, An efficient unstructured MUSCL scheme for solving the 2D shallow water equations. *Environmental Modelling & Software*, **66**, 131–152, 2015.

[10] J. Hou, Q. Liang, . Simons, R. Hinkelmann, A stable 2D unstructured shallow flow model for simulations of wetting and drying over rough terrains. *Computers & Fluids*, **82**, 132–147, 2013.

[11] A. Duran, F. Marche, Recent advances on the discontinuous Galerkin method for shallow water equations with topography source terms. *Computers & Fluids*, **101**, 88–104, 2014.

[12] S.W. Funke, C.C. Pain, S.C. Kramer, M.D. Piggott, A wetting and drying algorithm with a combined pressure/free-surface formulation for non-hydrostatic models. *Advances in Water Resources*, **34(11)**, 1483–1495, 2011.

[13] T. Kärnä, B. de Brye, O. Gourgue, J. Lambrechts, R. Comblen, V. Legat, E. Deleersnijder, A fully implicit wetting-drying method for DG-FEM shallow water models, with an application to the Scheldt Estuary. *Computer Methods in Applied Mechanics and Engineering*, **200(5-8)**, 509–524, 2011.

[14] Y. Li, F. Raichlen, Non-breaking and breaking solitary wave run-up. *Journal of Fluid Mechanics*, **456**, 295–318, 2002.

[15] E.T. Flouri, N. Kalligeris, G. Alexandrakis, N.A. Kampanis, C.E. Synolakis, Application of a finite difference computational model to the simulation of earthquake generated tsunamis. *Applied Numerical Mathematics*, **67**, 111–125, 2013.

[16] Yu.I. Shokin, S.A. Beisel, A.D. Rychkov, L.B. Chubarov, Numerical simulation of the tsunami runup on the coast using the method of large particles. *Mathematical Models and Computer Simulations*, **7(4)**, 339–348, 2015.

[17] A.A. Samarskii, *The theory of difference schemes*. USA: Marcel Dekker, Inc., 2001.

[18] G.S. Khakimzyanov, N.Yu. Shokina, Some notes on monotonicity preserving schemes. *Computational Technologies*, **17(2)**, 78–98, 2012. (in Russ.)

[19] N.Yu. Shokina, To the problem of construction of difference schemes on movable grids. *Russian Journal of Numerical Analysis and Mathematical Modelling*, **27(6)**, 603–626, 2012.

[20] S.P. Bautin, S.L. Deryabin, A.F. Sommer, G.S. Khakimzyanov, N.Yu. Shokina, Use of analytic solutions in the statement of difference boundary conditions on a movable shoreline. *Russian Journal of Numerical Analysis and Mathematical Modelling*, **26(4)**, 353–377, 2011.

[21] C.E. Synolakis, The runup of solitary waves. *Journal of Fluid Mechanics*, **185**, 523–545, 1987.

[22] S.A. Beizel, N.Yu. Shokina, G.S. Khakimzyanov, L.B. Chubarov, O.A. Kovyrkina, V.V. Ostapenko, On some numerical algorithms for computation of tsunami runup in the framework of shallow water model. I. *Computational Technologies*, **19(1)**, 40–62, 2014. (in Russ.)

[23] O.I. Gusev, N.Yu. Shokina, V.A. Kutergin, G.S. Khakimzyanov, Numerical modelling of surface waves generated by underwater landslide in a reservoir. *Computational Technologies*, **18(5)**, 74–90, 2013. (in Russ.)

[24] Yu.I. Shokin, S.A. Beisel, O.I. Gusev, G.S. Khakimzyanov, L.B. Chubarov, N.Yu. Shokina, Numerical modelling of dispersive waves generated by landslide motion. *Bulletin of the South Ural State University*, **7(1)**, 121–133, 2014. (in Russ.)

[25] B.L. Rozhdestvenskiy, N.N. Yanenko, *Systems of quasilinear equations and their application to gas dynamics*. Moscow: Nauka, 1978. (in Russ.)

[26] G. Pedersen, B. Gjevik, Run-up of solitary waves. *Journal of Fluid Mechanics*, **135**, 283–299, 1983.

[27] M.J. Cooker, P.D. Weidman, D.S. Bale, Reflection of a high-amplitude solitary wave at a vertical wall. *Journal of Fluid Mechanics*, **342**, 141–158, 1997.

[28] C.E. Synolakis, E.N. Bernard, V.V. Titov, U. Kanoglu, F.I. Gonzalez, Validation and verification of tsunami numerical models. *Pure and Applied Geophysics*, **165**, 2197–2228, 2008.

[29] J. Horrillo, S.T. Grilli, D. Nicolsky, V. Roeber, J. Zhang, Performance benchmarking tsunami models for NTHMP's inundation mapping activities. *Pure and Applied Geophysics*, **170(3-4)**, 1333–1359, 2015.